horticulturae

MDPI

Article

Integrated Transcriptomic and Metabolomic Analyses Reveal Root-Centered Regulatory Networks Conferring Cadmium Tolerance in *Salix*

Xiaomei Song [1,2], Ningqi Wang [3], Yuyi Zhang [4], Xudong He [5], Nan Guo [2,*] and Jun Tao [2,*]

[1] College of Art Design, Yangzhou Polytechnic Institute, Yangzhou 225107, China; 15995125668@163.com
[2] College of Horticulture and Landscape Architecture, Yangzhou University, Yangzhou 225009, China
[3] College of Resources and Environmental Sciences, Nanjing Agricultural University, Nanjing 210095, China; wangnq@njau.edu.cn
[4] Jiangsu Key Laboratory for Conservation and Utilization of Plant Resources, Institute of Botany, Jiangsu Province and Chinese Academy of Sciences (Nanjing Botanical Garden Memorial Sun Yat-Sen), Nanjing 210014, China; zhangyuyi@jib.ac.cn
[5] National Willow Engineering Technology Research Center, Jiangsu Academy of Forestry, Nanjing 211153, China; hxd_519@163.com
* Correspondence: nan.guo@yzu.edu.cn (N.G.); jtaoyzu@163.com or taojun@yzu.edu.cn (J.T.)

Abstract

Cadmium (Cd) is a major environmental pollutant due to its high mobility and persistence in soils, facilitating entry into the food chain and threatening ecosystems and human health. However, the mechanisms that enable *Salix* species, well adapted for Cd remediation, to both tolerate and accumulate Cd remain elusive. Here, two *Salix* genotypes with contrasting Cd tolerance were examined under control and Cd stress using integrated physiological, transcriptomic, and metabolomic analyses of roots and leaves. The Cd-tolerant genotype (*Salix suchowensis* P294) maintained biomass under Cd stress, whereas the Cd-sensitive genotype (*Salix sinopurpurea* × *Salix integra* P646) showed a ~17% reduction. P294 accumulated more Cd in its stems (132.76 mg kg^{-1}) and leaves (122.25 mg kg^{-1}) than P646 (93.54 and 56.24 mg kg^{-1}). Transcriptomics responses were stronger in roots, with 896 DEGs in P294 and 462 in P646, enriched in nitrogen metabolism, phenylpropanoid biosynthesis, and metal transport, whereas only 167 and 176 DEGs were detected in leaves for P294 and P646, respectively. Metabolomics revealed more altered metabolites in roots (125 in P294, 89 in P646), mainly organic acids, amino acids, and flavonoids, compared with leaves (46 and 66). RT-qPCR validated the root-specific upregulation of key detoxification and transport genes (*ABCA7*, *PRX72*, *GSTU1*, *GSTU4*, *ZIP1*). These results reveal a root-centered regulatory network underlying Cd accumulation and tolerance, integrating detoxification, redox homeostasis, and structural reinforcement, as well as providing valuable targets for genetic improvement of phytoremediation efficiency.

Keywords: cadmium; *Salix*; cadmium accumulation and resistance; transcriptomic analyses; metabolomic analyses

Check for updates

Academic Editors: Alessandra Carrubba and Michail Michailidis

Received: 5 February 2026
Revised: 5 April 2026
Accepted: 8 April 2026
Published: 10 April 2026

Copyright: © 2026 by the authors. Licensee MDPI, Basel, Switzerland. This article is an open access article distributed under the terms and conditions of the Creative Commons Attribution (CC BY) license.

1. Introduction

Cadmium (Cd) is a highly toxic, non-essential heavy metal that poses serious risks to plant growth, food safety, and human health, due to its high mobility in soils and its tendency to accumulate in plant tissues and enter the food chain [1,2]. Its widespread accumulation in soils, largely driven by mining, industrial discharge, and phosphate fertilizer

use, makes remediation of Cd-contaminated soils an urgent environmental challenge [3]. Among the available phytoremediation strategies, *Salix* has attracted particular attention due to its rapid growth, extensive root systems, high biomass yield, and remarkable Cd uptake and translocation capacity [4,5]. For instance, *Salix fragilis* has been reported to accumulate up to 150 mg Cd kg^{-1} dry weight while maintaining vigorous growth [6]. Meanwhile, Cd translocation factors of willows have exceeded 1.0 [7], exhibiting high efficiency in Cd phytoremediation. Field trials further demonstrated that multiple *Salix* clones such as *S. jiangsuensis* and *S. cheilophila* could remove more than 80% of Cd from contaminated soils within three years [8]. In addition to their ecological and forestry roles, *Salix* species are also widely used in horticultural systems, particularly in landscape design, urban greening, and environmental horticulture, where stress-tolerant woody plants are essential for sustainable management of marginal and contaminated soils [9–11]. These findings highlight *Salix* as a promising candidate for ecological restoration and sustainable Cd phytoremediation [12], which support their application as functional woody plants in horticultural systems facing soil contamination constraints.

The Cd-remediation potential of *Salix* is tightly dependent on its intrinsic Cd tolerance [13], displaying remarkable phenotypic variation in both Cd accumulation and tolerance [14]. In most genotypes, Cd accumulation and tolerance rarely co-occur; many genotypes survive by restricting Cd translocation to shoots, thereby minimizing damage to photosynthetic tissues [15]. Certain Cd hyperaccumulator plants can tolerate extremely high internal Cd concentrations, but these plants are mostly herbaceous genotypes with limited biomass that result in relatively low total Cd extraction efficiency [16]. In contrast, woody plants generally produce large biomass that should possess higher overall Cd removal potential, but they often suffer from growth inhibition under high Cd exposure [17]. Consequently, the phenotype with "high accumulation and high tolerance", which enables plants to extract Cd while maintaining their growth and biomass under Cd stress, is most desirable for phytoremediation. For example, a hydroponic screening of 39 *Salix* clones revealed leaf Cd concentrations ranging from 64 to 664 $\mu g \cdot g^{-1}$ and translocation factors spanning from 0.09 to 1.72 [18]. Such phenotypic diversity underscored the critical importance of identifying *Salix* phenotypes that combined high Cd accumulation with strong tolerance for effective phytoextraction. Hence, gaining insights into the physiological and molecular basis of these dual traits represents a key step toward optimizing *Salix* as a model genotype for Cd phytoremediation.

In model plants such as *Arabidopsis thaliana* and rice, the molecular mechanisms of Cd uptake, detoxification, and tolerance have been extensively characterized, providing well-established frameworks. These mechanisms include cell wall binding [19], chelation by phytochelatins and metallothioneins [20], vacuolar sequestration via tonoplast transporters [21] such as heavy-metal ATPase 3 (HMA3) [22], and xylem loading and unloading processes that regulate long-distance Cd distribution [23], all of which are involved in several functions such as sulfur metabolism, ion homeostasis, cell wall-related modifications, and flavonoid biosynthesis [24,25]. Such studies demonstrated that tolerance and accumulation were often achieved through finely tuned coordination between transporter activity, metal chelation, and redox homeostasis [26]. However, mechanistic insights into Cd responses of *Salix* remain fragmentary. Existing studies have focused on phenotypic and physiological assessments, reporting significant genotypic variation in Cd accumulation, translocation, and biomass maintenance under stress [27,28]. Functional studies on *Salix* or related systems have demonstrated that individual genes can influence Cd handling. For example, overexpression of *Salix matsudana Koidz* SmZIP in transgenic tobacco increased Cd accumulation and altered subcellular distribution, while expression of *Salix suchowensis* SsIRT9 enhanced Cd uptake and modified metal homeostasis [29,30].

Transcriptomic analyses comparing contrasting willow genotypes have identified candidate transporters such as iron-regulated transporter and heavy-metal ATPases, as well as the glutathione pathway, which likely contribute to differential Cd accumulation and tolerance [31]. However, the integrated transcriptional and metabolic programs that allow certain *Salix* genotypes to simultaneously tolerate and accumulate high Cd remain poorly understood. In particular, it is unclear whether root-localized defenses alone can explain the tolerant phenotype, or whether coordinated systemic adjustments between roots, stems, and leaves contribute to maintaining growth under Cd stress. This lack of integrative multi-omics evidence limits our understanding of how *Salix* achieves the rare "high-accumulation and high-tolerance" trait.

To address these knowledge gaps, we selected two representative *Salix* genotypes with contrasting Cd accumulation and tolerance profiles: *Salix sinopurpurea* × *Salix integra* P646, a low-Cd-accumulating and Cd-susceptible genotype [32], and *Salix suchowensis* P294, a high-Cd-accumulating and Cd-tolerant genotype [33]. We conducted a hydroponic experiment comparing the Cd-susceptible P646 and the Cd-tolerant P294 under control (0 μM Cd) and Cd stress (20 μM Cd) conditions, which represent a critical toxicity threshold at which growth inhibition and Cd-induced physiological stress become evident [28], and measured growth performance, plant biomass, and organ-specific Cd accumulation indices. We then integrated transcriptomic and metabolomic analyses in both roots and leaves to investigate why a high-Cd-accumulating *Salix* can simultaneously maintain tolerance. This multi-dimensional approach allows us to pinpoint key tissues and regulatory mechanisms underlying Cd tolerance, resolve organ-specific adaptation strategies, and provide mechanistic insights into the phytoremediation potential of representative *Salix* genotypes.

2. Materials and Methods

2.1. Plant Materials and Hydroponic Culture

Two *Salix* genotypes (*Salix suchowensis* P294 [33] and *Salix sinopurpurea* × *Salix integra* P646 [32]) with contrasting Cd tolerance were used in this study. Cuttings (10 to 12 cm in length, 0.8 cm in diameter) were pre-rooted in half-strength Hoagland nutrient solution for two weeks under controlled-growth conditions (25 ± 2 °C, 16 h light/8 h dark photoperiod, 60% relative humidity). After establishment, eleven uniform and healthy rooted cuttings per genotypes were selected and transferred to a full-strength Hoagland solution containing either 0 μM Cd (control) or 20 μM Cd, supplied as $CdCl_2 \cdot 2.5H_2O$, for two weeks [28]. Plants were selected based on uniform growth (similar height and leaf number), absence of visible damage or disease, and consistent establishment in the hydroponic system. Individuals meeting these criteria were randomly chosen to ensure representativeness and minimize selection bias. The nutrient solution was renewed every three days and continuously aerated. *Salix* plants were harvested after 2 weeks of Cd treatment for phenotypic, physiological, transcriptomic, and metabolomic analyses, following the protocol as previously reported [28]. For growth parameter assessment and Cd concentration determination, five independent biological replicates were used for each treatment, with each replicate consisting of one individual plant grown under identical hydroponic conditions. In details, plant height (cm), root length (cm), and fresh weight (g) were measured at harvest using a ruler and digital caliper. Tissues were oven-dried at 105 °C for 30 min and then at 70 °C until constant weight for biomass determination. For transcriptomic and metabolomic analyses, six individual plants per treatment were sampled. To better capture genotype-level responses while minimizing individual variability and ensuring sufficient RNA yield, samples were pooled pairwise prior to RNA extraction (two plants per pooled sample), resulting in three pooled biological replicates

(n = 3) per treatment. All subsequent transcriptomic analyses were performed on these pooled samples, with each replicate treated as an independent biological unit.

2.2. Cd Concentration Analysis

Five of the harvested *Salix* plants were separated into roots, stems, and leaves, which were subsequently used for Cd analysis. Cd concentrations were determined following the ICP OES protocols [28] (iCAP6300, Thermo Scientific, Waltham, MA, USA). Translocation factors (TFs) were calculated as the ratio of Cd concentration in stems or leaves to that in roots.

2.3. RNA Extraction, Library Preparation, and Sequencing for Transcriptomic Analyses

Total RNA was extracted from root and leaf for each treatment with three biological replicates per treatment using the Trizol reagent (Invitrogen, Carlsbad, CA, USA) according to the manufacturer's instructions. RNA concentration and purity were assessed using a NanoDrop 2000 spectrophotometer (Thermo Fisher Scientific, Waltham, MA, USA), and integrity was examined using an Agilent 2100 Bioanalyzer (Agilent Technologies, Santa Clara, CA, USA). High-quality RNA (RIN $\geq$ 7.0, OD260/280 between 1.8 and 2.2) was used for library construction. Poly(A) mRNA was enriched using oligo(dT) magnetic beads and fragmented. First-strand cDNA was synthesized using random primers, followed by second-strand synthesis. After end repair, A-tailing, and adapter ligation, libraries were PCR-amplified. Library quality and size distribution were assessed using Qubit 2.0 and the Agilent Bioanalyzer (Agilent Technologies, Shanghai, China). Sequencing was performed on the Illumina NovaSeq 6000 platform (paired-end 150 bp) at Metware Biotechnology Co., Ltd. (Wuhan, China). Raw sequencing reads were processed with fastp [34] to remove adapter sequences, reads with >10% N bases, and low-quality reads. Clean reads were aligned to the *Salix* reference genome (*Salix suchowensis*, ncbi genome assembly ASM2903076v1) using HISAT2 (v2.2.1) [35]. Across all samples, a proportion of clean reads were successfully mapped to the reference genome, with uniquely mapped reads accounting for 92.65–94.10% of total reads. Transcript assembly and quantification were conducted with StringTie (V3.0.3) [36], and expression levels were normalized as FPKM for further analysis. For differential expression analysis, gene-level raw read counts were generated from the aligned reads and used as input for DESeq2, following the standard workflow. Functional annotation were performed against the GO (2024-01-17) and KEGG databases (Release 111.0), and pathways with q $\leq$ 0.05 were considered significantly enriched, where q-values were obtained using the Benjamini–Hochberg false discovery rate (FDR) correction method. The transcriptome analysis was conducted using the pipeline in CFViSA [37].

2.4. RT-qPCR Validation

To validate RNA-Seq results, five DEGs were selected for RT-qPCR analysis: *ABCA7* (ABC transporter A family member 7; OIU76_000668), *PRX72* (peroxidase 72; OIU76_024379), *GSTU1* and *GSTU4* (glutathione S-transferases; OIU76_013259 and novel.1736), and *ZIP1* (zinc transporter 1; OIU76_012093). These genes represent key functional categories including metal transport process, redox homeostasis, and glutathione metabolism. Cuttings of each genotype (about 0.8 cm in diameter, 12 cm in length) were initially cultured in a plastic tank containing 15 L of water for 2 weeks, then transferred to 1/4-strength Hoagland's nutrient solution for an additional 2 weeks. Three uniform cuttings of each genotype were subjected to either 20 μM Cd or a Cd-free control for 2 weeks. After Cd exposure, roots were harvested for gene expression analysis.

Total RNA was extracted using TaKaRa MiniBEST Plant RNA Extraction Kit (TaKaRa, Dalian, China). RNA concentration and purity were assessed using the UNano-1000

Micro-volume Spectrophotometer (YoMim, Hangzhou, China). First-strand cDNA was synthesized using the EasyScript® All-in-One First-Strand cDNA Synthesis SuperMix for qPCR Kit (TransGen, Beijing, China). RT-qPCR was performed with PerfectStart® Green qPCR SuperMix (TransGen, Beijing, China) on the BioRad CFX Connect Real-Time PCR Detection System (BioRad, Hercules, CA, USA). Gene-specific primers were designed based on the *Salix suchowensis* genome and listed in Table S1. Relative gene expression levels were normalized to the reference genes, *αTUB* or *EF1α*, and presented as $2^{(-\Delta CT)}$ [38].

2.5. Targeted Metabolomic Profiling and Analysis

Root and leaf samples were freeze-dried with a lyophilizer (Scientz-100F, Ningbo Scientz Biotechnology Co. Ltd., Ningbo, China), finely ground (MM 400, Retsch, Haan, Germany), and 50 mg of powder was extracted with 1.2 mL of pre-cooled 70% methanol containing internal standards. This solvent system was selected for its established efficacy in extracting polar and semi-polar metabolites (amino acids, organic acids, phenolics, and alkaloids) central to metal stress responses, while pre-cooling minimizes enzymatic degradation [39]. Quality control (QC) measures included solvent blank injections (70% methanol) to monitor background contamination, and we pooled QC sample injections (mixed extracts from all samples) at regular intervals (every 10 samples) to assess instrument stability throughout the analytical run. Metabolite features with coefficient of variation (CV) > 30% in QC samples were filtered out to ensure reproducibility. No missing value imputation was required as no metabolites fell below the detection limit. The extracts were vortexed, centrifuged at 12,000 rpm for 3 min, and filtered through 0.22 μm membranes. Metabolite separation was performed on an ExionLC™ AD UPLC system (SCIEX, Marlborough, MA, USA) equipped with an Agilent SB-C18 column (1.8 μm, 2.1 mm × 100 mm, Agilent Technologies, Shanghai, China). The mobile phases consisted of water with 0.1% formic acid (A) and acetonitrile with 0.1% formic acid (B), using a gradient elution program at 0.35 mL/min and 40 °C. The effluent was introduced into a QTRAP-MS/MS system (SCIEX, Marlborough, MA, USA) with an electrospray ionization source operating in both positive and negative modes.

Metabolites were identified by comparing retention times and MS/MS spectra against an in-house MWDB database (v2.17.0) and KEGG databases (Release 111.0). KEGG annotation and pathway enrichment were performed to identify significantly enriched metabolic pathways based on hypergeometric tests, with q-values obtained using false discovery rate (FDR) correction. Peak areas were normalized by unit variance (UV) scaling (z-score transformation) for multivariate analysis. The metabolomic analysis was conducted using the pipeline in CFViSA (v2025) [37]. In detail, multivariate statistical analyses, including principal component analysis (PCA) and orthogonal partial least squares discriminant analysis (PLS-DA), were conducted in R with the MetaboAnalystR package (v4.0) [40]. PLS-DA was performed with internal cross-validation (leave-one-out) and permutation testing (n = 200 permutations), yielding $R^2X = 0.732$ and $Q^2 = 0.976$ with model significance confirmed ($p < 0.001$).

2.6. Statistical Analysis

Statistical significance in phenotypes between treatments was determined using Student's t-test or Wilcoxon rank-sum test as appropriate, with a threshold of $p < 0.05$. Two-way permutational multivariate analysis of variance (PERMANOVA) was conducted in R (version 4.3.0) using the *vegan* package (v2.7-1) [41] to determine the effects from genotype, Cd stress, and their interaction based on Euclidean distance. Pairwise PERMANOVA was conducted to detemine pairwise differences among samples using *pairwiseAdonis* package (https://github.com/pmartinezarbizu/pairwiseAdonis, accessed on 19 October 2025). Dif-

ferentially expressed genes (DEGs) and metabolites (DEMs) were identified using DESeq2 (v1.45.3) [42] with thresholds of abosolute value of $\log_2$ fold change > 1.5 and FDR (adjusted *p* value) < 0.05.

3. Results

3.1. Phenotypic Differences Between Cd-Tolerant and Cd-Susceptible Salix Genotypes Under Cd Stress

Under hydroponic conditions with Cd stress (20 µM), the two *Salix* genotypes exhibited distinct phenotypic responses. The genotype P294 (Figure 1A, right panel) displayed enhanced tolerance characteristics compared to the Cd-susceptible genotype P646 (Figure 1A, left panel). Specifically, the Cd-tolerant genotype P294 developed a more robust root system, with significantly longer root length under Cd stress. Although both genotypes exhibited an approximately 20% reduction in plant height under Cd stress ($p = 0.004$ for P646 and $p < 0.001$ for P294), Cd stress markedly reduced root length in P646 by 18.45% ($p = 0.016$), whereas no significant change was observed in the Cd-tolerant genotype P294 (+5.89%, $p = 0.304$). Plant biomass significantly decreased by 17.25% for P646 ($p = 0.014$) under Cd stress, yet P294 was not significantly affected (−13.93%, $p = 0.282$, Figure 1B).

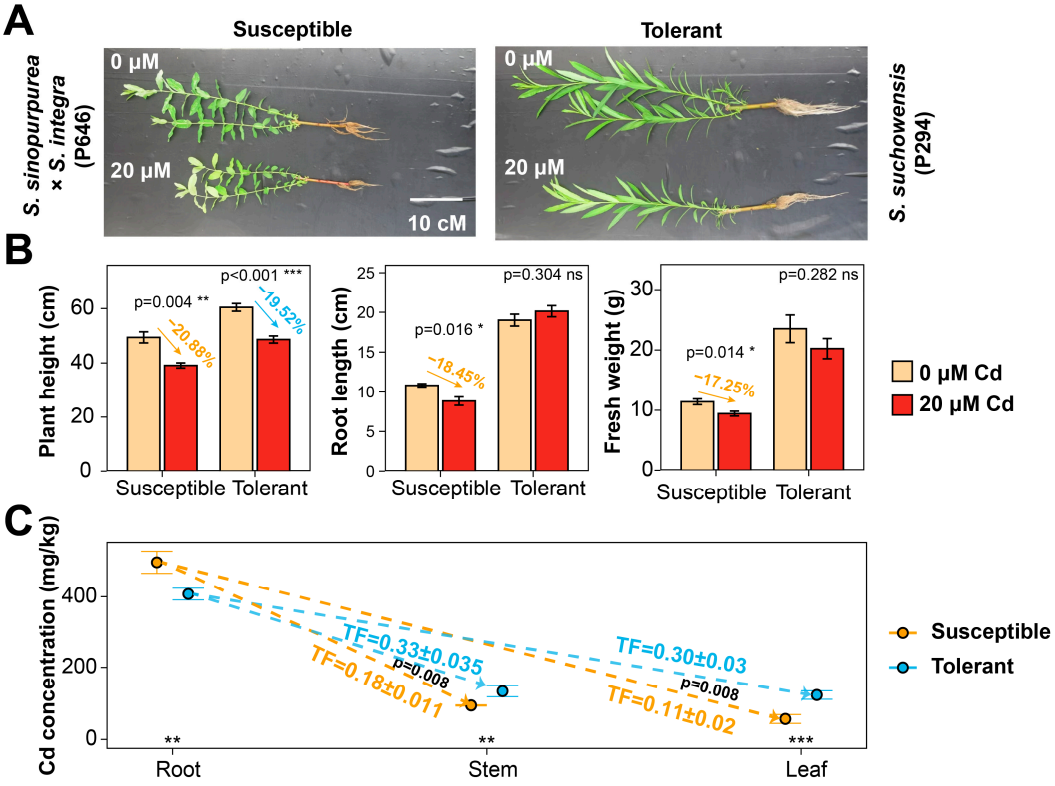

Figure 1. Phenotypic differences between two *Salix* genotypes (P294 and P646) under cadmium stress. (**A**) Representative images of the Cd-sensitive genotype P646 and Cd-tolerant genotype P294 grown hydroponically under 0 µM Cd and 20 µM Cd stress for 2 weeks. (**B**) Comparison of growth performance under Cd stress between two genotypes, including plant height (cm), root length (cm), and fresh weight (g). Values represent mean ± standard deviation (SD). (**C**) Cd concentrations in roots, stems, and leaves, along with corresponding translocation factors (TFs) in both genotypes. Dots indicate Cd concentrations in each organ, with error bar representing SD of Cd concentrations ($n = 5$). Connecting lines represent Cd translocation from root to stem and to leaf. Numeric labels above the lines show the mean ± SD of the translocation factors ($n = 5$). Asterisks denote significance levels based on *t*-tests: ns, $p > 0.05$, *, $p < 0.05$; **, $p < 0.01$, ***, $p < 0.001$. Colors indicate genotype identity: yellow for the Cd-tolerant genotype (P294); blue for the Cd-sensitive genotype (P646).

Tissue Cd measurements revealed contrasting accumulation and partitioning strategies between the genotypes (Figure 1C). P646 roots accumulated significantly more Cd (497.57 mg/kg) than P294 (407.64 mg/kg, +22.06%, $p = 0.0012$), whereas P294 accumulated markedly higher Cd in stems (132.76 mg/kg, +29.54%, $p = 0.0045$) and leaves (122.25 mg/kg, +53.60%, $p < 0.0001$) compared with P646 (93.54 mg/kg and 56.24 mg/kg, respectively). Consistently, Cd translocation factors (TFs) were significantly higher in P294, with the root-to-stem TF reaching 0.33 ($p = 0.008$, Mann–Whitney test), and the root-to-leaf TF also elevated (reaching 0.30, $p = 0.008$, Figure S1 and Figure 1C).

Taken together, these results demonstrated that the Cd-tolerant genotype P294 maintained better growth performance under Cd stress, primarily through sustaining root development and biomass production. Moreover, P294 exhibited a distinctive Cd redistribution strategy by limiting Cd retention in roots and promoting its efficient translocation to aerial parts. This phenotype not only alleviates root Cd toxicity but also enhances whole-plant Cd uptake and allocation, highlighting the dual characteristics of P294 as both a Cd-tolerant and Cd-accumulative genotype.

3.2. Transcriptional Reprogramming of Antioxidant, Secondary Metabolism, and Transport Pathways Associated with Cd Tolerance in Salix Roots

To investigate the differences in transcriptional strategies between the two *Salix* genotypes under Cd stress, we first analyzed RNA-seq data from roots and leaves. Exposure to 20 μM Cd induced significant transcriptomic alterations in both genotypes and tissues (Figure 2A), with roots exhibiting more pronounced responses than leaves. Principal component analysis (PCA) revealed distinct expression patterns across genotypes and treatments in roots ($R^2 = 0.52$, $p < 0.001$ for genotype, $R^2 = 0.27$, $p < 0.001$ for Cd stress, PERMANOVA), whereas leaf transcriptomes showed less separation. Pairwise comparisons showed that the Cd-tolerant genotype exhibited a stronger transcriptomic shift ($R^2 = 64.68\%$) than the Cd-susceptible genotype ($R^2 = 56.89\%$) in roots under Cd exposure, suggesting stronger transcriptional responses to Cd stress. In contrast, transcriptional variance in leaves was comparatively modest, with genotype and Cd stress explaining 37.15% ($p < 0.001$) and 20.36% ($p = 0.006$, Figure 2A), respectively. Differential expression analyses further supported these patterns (Figure 2B). In roots, the Cd-tolerant genotype exhibited 896 DEGs (621 upregulated and 275 downregulated), nearly double the number detected in the Cd-susceptible genotype (462 DEGs, with 316 upregulated and 146 downregulated). In contrast, the number of DEGs in leaves was similar between genotypes: 167 DEGs (110 up- and 57 downregulated) in the tolerant genotype and 176 DEGs (144 up- and 32 downregulated) in the susceptible genotype (Figure 2B and Table S2). These results indicated that the tolerant genotype activated a more extensive transcriptional changes in roots to counteract Cd stress.

We next conducted KEGG enrichment analysis and compared the differences in their enriched KEGG functions between two genotypes (Figure 2C). In roots, both genotypes exhibited significant enrichment of Cd-responsive pathways but with divergent strengths. The Cd-tolerant genotype showed higher enrichment in nitrogen metabolism (enrichment factor = 4.47, q = 0.0059), cysteine and methionine metabolism (2.39, q = 0.027), ABC transporter activity (2.89, q = 0.0059), and MAPK signaling pathway–plant (1.80, q = 0.018), while the susceptible genotype exhibited lower enrichment for the same functions (nitrogen metabolism: 1.86, q = 0.889; cysteine and methionine metabolism: 1.70, q = 0.601; ABC transporter activity: 1.92, q = 0.438; MAPK signaling: 1.30, q = 0.774). Phenylpropanoid biosynthesis was strongly enriched in both genotypes but was more pronounced in tolerant roots (3.57, $q = 7.21 \times 10^{-8}$) compared with susceptible roots (3.37, $q = 3.69 \times 10^{-4}$). Conversely, glutathione metabolism was more strongly enriched in susceptible roots (7.45, $q = 7.14 \times 10^{-10}$) than in tolerant roots (3.06, q = 0.0059, Figure 2C, above panel). These

transcriptomic shifts were associated with enrichment of nutrient and sulfur metabolism, structural-related pathways, and transporter-related functions in tolerant roots, while susceptible roots over-activated glutathione pathways yet failed to prevent Cd accumulation. In leaves, a partially reversed pattern was observed. The tolerant genotype exhibited higher enrichment in glutathione metabolism (2.99, q = 0.545), cysteine and methionine metabolism (4.79, q = 0.101), and nitrogen metabolism (6.28, q = 0.528), whereas the tolerant genotype showed stronger enrichment in phenylpropanoid biosynthesis (5.29, q = 0.016), ABC transporter activities (4.89, q = 0.110), and MAPK signaling pathway–plant (3.04, q = 0.070, Figure 2C, bottom panel). Together, these results indicated that Cd-tolerant roots mainly activated nitrogen, sulfur, and transporter-related pathways for Cd stress defense.

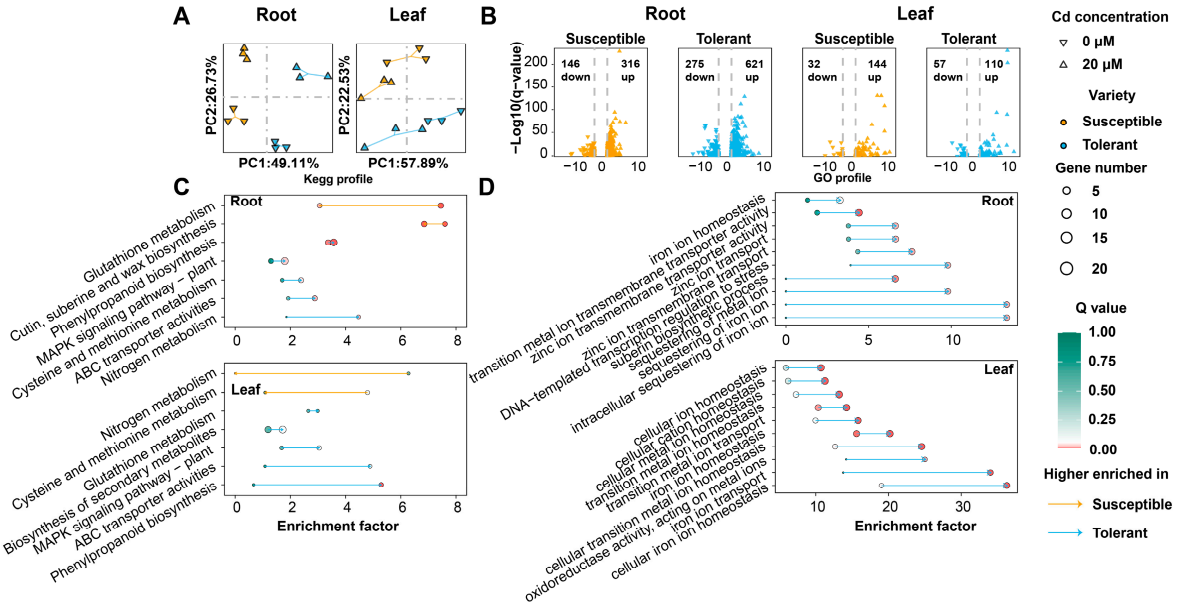

Figure 2. Transcriptomic analysis reveals differential gene expression patterns in roots and leaves between Cd-tolerant and Cd-susceptible *Salix* genotypes. (**A**) Principal component analysis (PCA) illustrating transcriptomic variation in roots and leaves of the two genotypes under 0 μM Cd and 20 μM Cd treatments. (**B**) Differentially expressed genes (DEGs) identified by DESeq2 for roots and leaves of each genotype between 0 μM Cd and 20 μM Cd treatments. DEGs were defined as those with $|\log_2$ fold change$| > 1.5$ and q-value < 0.05. (**C**) KEGG pathway enrichment analysis showing transcriptomic differences in response to Cd stress between the two genotypes for roots (**upper panel**) and leaves (**lower panel**). (**D**) GO enrichment analysis showing functional differences in response to Cd stress between the two genotypes for roots (**upper panel**) and leaves (**lower panel**). Bubble size indicates the number of enriched DEGs per pathway, and color represents enrichment significance (q-value). Arrows indicate the direction of difference in functional pathways from the Cd-susceptible (arrow start, yellow) to the Cd-tolerant (arrow end, blue) genotype.

GO enrichment analysis further revealed pronounced differences between the two genotypes in roots (Figure 2D, above panel). The tolerant genotype exhibited strong enrichment in metal-related processes, including zinc ion transmembrane transport (GO:0071577, enrichment factor = 7.62, q = 0.0035), zinc ion transport (GO:0006829, 6.64, q = 0.0075), and zinc ion transmembrane transporter activity (GO:0005385, 6.62, q = 0.0075), all of which were only weakly enriched in the susceptible genotype (3.78, q = 0.529; 3.77, q = 0.529; 4.34, q = 0.476, respectively). In addition, tolerant roots showed significant enrichment in iron ion homeostasis (GO:0055072, 3.27, q = 0.045), intracellular iron ion sequestration (GO:0006880, 13.36, q = 0.0029), and general metal ion sequestration (GO:0051238, 9.80, q = 0.0087), which were absent in the susceptible counterpart. Tolerant roots also displayed enrichment in transition metal ion transmembrane transporter activity (GO:0046915,

4.41, q = 9.0 × 10^{-4}) and regulation of DNA-templated transcription in response to stress (GO:0043620, 9.80, q = 0.0087). By contrast, the susceptible genotype only showed weak or non-significant enrichment of similar terms. Notably, the suberin biosynthetic process (GO:0010345) was highly enriched in tolerant roots (6.61, q = 0.0014) but absent in susceptible roots, suggesting enhanced structural barrier formation. In leaves, both genotypes exhibited significant enrichment of ion homeostasis-related processes, yet tolerant leaves consistently displayed stronger effects (Figure 2D, bottom panel). The tolerant genotype was enriched for transition metal ion homeostasis (GO:0055076, 14.22, q = 1.40 × 10^{-9}), iron ion homeostasis (GO:0055072, 20.19, q = 1.40 × 10^{-9}), and cellular iron ion homeostasis (GO:0006879, 36.27, q = 8.62 × 10^{-10}), whereas enrichment in susceptible leaves was weaker (10.34, q = 1.76 × 10^{-5}; 15.61, q = 4.59 × 10^{-6}; 19.04, q = 1.05 × 10^{-3}, respectively). Similarly, transition metal ion transport (GO:0000041) and oxidoreductase activity acting on metal ions (GO:0016722) were markedly stronger in tolerant leaves (15.82, q = 3.99 × 10^{-7}; 25.01, q = 6.11 × 10^{-5}) compared to susceptible ones (9.96, q = 1.80 × 10^{-3}; 14.18, q = 0.022). The tolerant genotype also showed enrichment in broader categories such as cellular ion homeostasis (GO:0006873, 10.72, q = 1.23 × 10^{-7}) and cellular metal ion homeostasis (GO:0006875, 13.22, q = 1.74 × 10^{-8}), both stronger than in susceptible leaves (5.91, q = 0.0053; 7.28, q = 0.0019). These molecular functions correspond well with phenotypic data, where tolerant leaves accumulated more Cd and exhibited higher transfer coefficients from root to stem and to leaf.

To confirm the reliability of transcriptomic results, we validated the expression patterns of five representative DEGs by RT-qPCR, including *ABCA7* (ABC transporter), *PRX72* (peroxidase), *GSTU1* and *GSTU4* (glutathione S-transferases), and *ZIP1* (zinc transporter). They were selected based on their functional relevance to Cd transport, redox homeostasis, and detoxification pathways identified in our transcriptomic analysis (Figure 2, Table S2). All five genes showed significant Cd-induced upregulation in both genotypes, consistent with RNA-Seq results (Figures 2 and 3). The expression trends were corroborated using two independent reference genes (*EF1α* and *αTUB*; Figure 3 and Figure S2), supporting the technical reliability of our transcriptomic dataset.

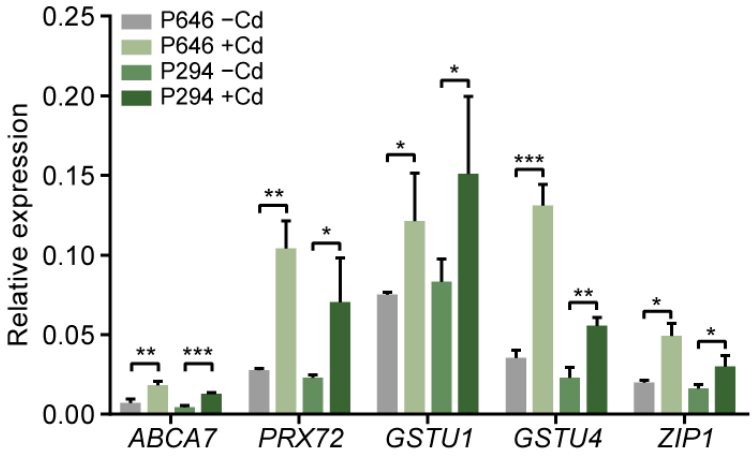

Figure 3. The expression patterns of differentially expressed genes (DEGs) identified by RNA-Seq using RT-qPCR. Cuttings of genotypes P294 and P646 were exposed to either 20 µM Cd (+Cd) or Cd-free conditions (−Cd) for 2 weeks. Roots were harvested for RT-qPCR analysis. The willow reference gene *EF1α* was used as an internal control. Data are presented as means ± SD (n = 3). Asterisks indicate significant differences determined by Student's t-test. *, $p < 0.05$; **, $p < 0.01$, ***, $p < 0.001$. ABCA7, ABC transporter A family member 7; PRX72, peroxidase 72; GSTU1, glutathione S-transferase 1; GSTU4, glutathione S-transferase 4; ZIP1, zinc transporter 1.

Taken together, transcriptomic analyses revealed pronounced differences in Cd-responsive gene expression patterns between the two *Salix* genotypes. Compared with the Cd-susceptible genotype, the Cd-tolerant genotype displayed a broader range and higher magnitude of differentially expressed genes, particularly in roots. Genes associated with amino acid metabolism, redox-related functions, cell wall-associated processes, and metal ion transport and homeostasis were more frequently and strongly enriched in the tolerant genotype across both roots and leaves.

3.3. Enhanced Detoxification and Defense-Related Metabolic Pathways Define Cd Tolerance in Salix Roots

To investigate the metabolic responses of *Salix* to Cd stress, we systematically profiled the root and leaf metabolomes of Cd-tolerant and Cd-susceptible genotypes under 0 μM Cd and 20 μM Cd treatments. Consistent with transcriptomic results, metabolic responses were markedly stronger in roots than in leaves, indicating that roots showed stronger metabolic responses to Cd stress compared with leaves. In roots, the dominant metabolite classes were flavonoids, phenolic acids, and alkaloids, which together accounted for more than 50% of the total metabolite pool (Figure 4A). Cd exposure significantly increased alkaloid accumulation in both genotypes ($p = 0.020$ for the tolerant and $p = 0.018$ for the susceptible genotype, Wilcoxon test). However, distinct genotype-specific patterns were observed: tannins were selectively upregulated in the susceptible genotype ($p = 0.048$), whereas the tolerant genotype uniquely exhibited elevated levels of amino acids and derivatives ($p = 0.0077$) and organic acids ($p = 0.0042$), accompanied by a reduction in flavonoids ($p = 0.018$) under 20 μM Cd treatment (Figure 4A). In leaves, flavonoids and phenolic acids were the major classes. While the susceptible genotype showed comparable proportions of flavonoids (26.83%) and phenolic acids (27.45%), the tolerant genotype displayed a clear bias toward flavonoids (42.21%) over phenolic acids (19.48%), highlighting intrinsic metabolic differences between genotypes.

Multivariate analyses further supported these patterns. PLS-DA and PERMANOVA revealed that root metabolomes of both genotypes responded strongly to Cd stress, whereas leaf profiles were dominated by ecotypic differences (Figure 4B). In roots, genotype explained 69.29% of the variance ($p < 0.001$), and Cd stress contributed 15.67% ($p = 0.002$). Within each genotype, Cd stress accounted for 60.61% of the variation in the susceptible genotype ($p < 0.001$) and 61.81% in the tolerant genotype ($p < 0.001$), indicating comparable but robust Cd-induced metabolic reprogramming. By contrast, leaf metabolomes were largely shaped by genotype identity ($R^2 = 93.11\%$, $p < 0.001$), with Cd treatment explaining only a minor fraction of the variation ($R^2 = 2.89\%$, $p = 0.083$), suggesting that leaf metabolic differences primarily reflect inherent genetic backgrounds rather than inducible responses.

Differential expression analysis further highlighted these ecotypic contrasts (Figure 4C and Table S3). In roots, the tolerant genotype exhibited 125 differentially expressed metabolites (DEMs; 79 upregulated and 46 downregulated), whereas the susceptible genotype showed 89 DEMs (39 upregulated and 50 downregulated). In leaves, fewer DEMs were detected overall, with the tolerant genotype showing 45 DEMs (22 upregulated and 23 downregulated) and the susceptible genotype showing 66 DEMs (33 upregulated and 33 downregulated). Collectively, these results underscored that Cd tolerance in *Salix* was associated with distinct root metabolic adjustments, while leaf metabolomes primarily reflected constitutive differences between genotypes.

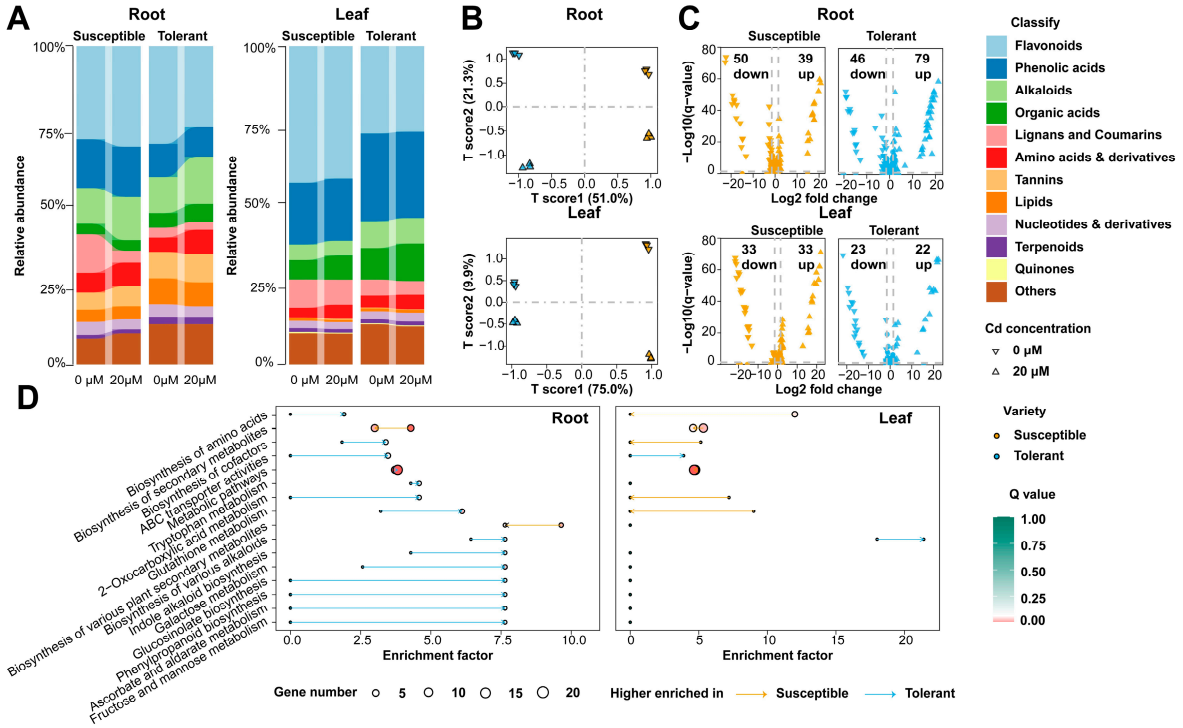

Figure 4. Metabolomic analysis reveals differences in root metabolites between Cd-tolerant and Cd-susceptible *Salix* genotypes. (**A**) Composition of root metabolite profiles in the Cd-tolerant and Cd-susceptible genotypes under 0 μM Cd and 20 μM Cd treatments in both roots (**left panel**) and leaves (**right panel**). (**B**) Partial least squares discriminant analysis (PLS-DA) illustrating the overall differences in metabolomes between the two genotypes under 0 μM Cd and 20 μM Cd conditions in both roots (**upper panel**) and leaves (**lower panel**). (**C**) Differentially expressed metabolites (DEMs) identified by DESeq2 for roots (**upper panel**) and leaves (**lower panel**) of each genotype between 0 μM Cd and 20 μM Cd treatments. DEMs were defined as those with $|\log_2$ fold change$| > 1.5$ and q-value < 0.05. (**D**) KEGG pathway enrichment analysis showing metabolomic differences in response to Cd stress between the two genotypes for roots (**left panel**) and leaves (**right panel**). Bubble size indicates the number of enriched DEMs per pathway, and color represents enrichment significance (q-value). Arrows indicate the direction of difference in functional pathways from the Cd-susceptible (arrow start, yellow) to the Cd-tolerant (arrow end, blue) genotype.

To further characterize the metabolic alternation underlying Cd responses, KEGG pathway enrichment analysis was performed based on DEMs in roots and leaves (Figure 4D). In roots, both genotypes exhibited enrichment in broad metabolic categories, but the magnitude of enriched pathways differed substantially. The tolerant genotype showed much stronger and broader enrichment than the susceptible genotype, with metabolic pathways (23 DEMs) and biosynthesis of secondary metabolites (11 DEMs) as the most significantly enriched categories, both exceeding the corresponding enrichments in the susceptible genotype (11 DEMs and 9 DEMs, respectively). Beyond these general categories, the tolerant genotype displayed specific activation of stress- and detoxification-related pathways, including glutathione metabolism (4 DEMs versus 1 DEM with no significance in susceptible roots), ABC transporter activities (5 DEMs while absent in susceptible roots), and ascorbate and aldarate metabolisms (2 DEMs, but not enriched in the susceptible genotype). In addition, specialized secondary metabolism pathways (such as phenylpropanoid biosynthesis, indole alkaloid biosynthesis, glucosinolate biosynthesis) and biosynthesis of various alkaloids were significantly enriched only in tolerant roots, while in the susceptible genotype, enrichment of these pathways was weak or absent. Collectively, these results indicated that metabolic changes in tolerant roots were broader and involved a wider range of metabolic

pathways. In leaves, enrichment was less extensive than in roots, but consistent ecotypic differences were still observed. In both genotypes, general enrichment was detected in metabolic pathways and biosynthesis of secondary metabolites. However, the susceptible genotype showed stronger enrichment in biosynthesis of amino acids and marginal significance in biosynthesis of various alkaloids, whereas the tolerant genotype displayed a higher enrichment score in biosynthesis of various alkaloids but no significant enrichment for glutathione metabolism or amino acid metabolism. Thus, while leaf responses were relatively limited compared to roots, the tolerant genotype still showed preferential activation of alkaloid biosynthesis, in contrast to the susceptible genotype that more strongly engaged amino acid metabolism. Together, these results demonstrated that Cd-induced metabolic adjustments in *Salix* were predominantly root-centered, where the tolerant genotype exhibited both stronger enrichment and broader activation of detoxification- and defense-related metabolic pathways, while leaf responses remained comparatively restricted and primarily reflected secondary metabolic processes.

3.4. Integrated Transcriptomic and Metabolomic Analysis Reveals Coordinated Patterns Associated with Cd Tolerance in Salix

Integration of transcriptomic and metabolomic datasets revealed four major patterns associated with Cd tolerance in *Salix*. First, secondary metabolism and structural reinforcement were prominent in tolerant roots. Genes involved in phenylpropanoid biosynthesis and suberin formation were upregulated, while metabolites such as phenolic acids, alkaloids, and glucosinolate-related compounds were enriched, suggesting potential changes related to apoplastic barrier formation that limited Cd influx (Figure 5, box 1). Second, redox regulation and antioxidant metabolism were enhanced in tolerant roots. Transcriptomic enrichment in cysteine and methionine metabolism and glutathione-related pathways was accompanied by the accumulation of amino acids and organic acids in metabolomic data, including γ-glutamylcysteine, cysteinyl-glycine, and ascorbate-related metabolites. These coordinated changes indicated reinforced redox buffering and antioxidant defense that supported root growth under Cd stress for the Cd tolerance genotype (Figure 5, box 2). Third, metal ion transport and detoxification were strengthened. ABC transporters and ion homeostasis-related GO terms were significantly enriched in tolerant roots, while elevated organic acids such as citrate and malate in metabolomic profiles imply improved Cd chelation and efflux capacity. These processes corresponded with lower Cd accumulation in tolerant roots and higher Cd translocation to stems and leaves (Figure 5, box 3). Finally, the integrated analysis revealed a coordinated root–leaf functional partitioning in the Cd-tolerant genotype. Phenotypically, tolerant plants maintained stable biomass and exhibited higher Cd translocation factors compared with the susceptible genotype, suggesting efficient systemic distribution of absorbed Cd. At the molecular level, tolerant roots predominantly facilitated Cd uptake and chelation through enhanced organic acid synthesis and ABC transporter activation, while leaves engaged in metabolic adjustment involving phenylpropanoid and flavonoid pathways, likely contributing to Cd stabilization and detoxification in aerial tissues. This spatial response pattern between below- and aboveground organs may contribute to differences in Cd distribution and physiological responses under Cd stress, reflecting an integrated tolerance strategy at the whole-plant level (Figure 5, box 4).

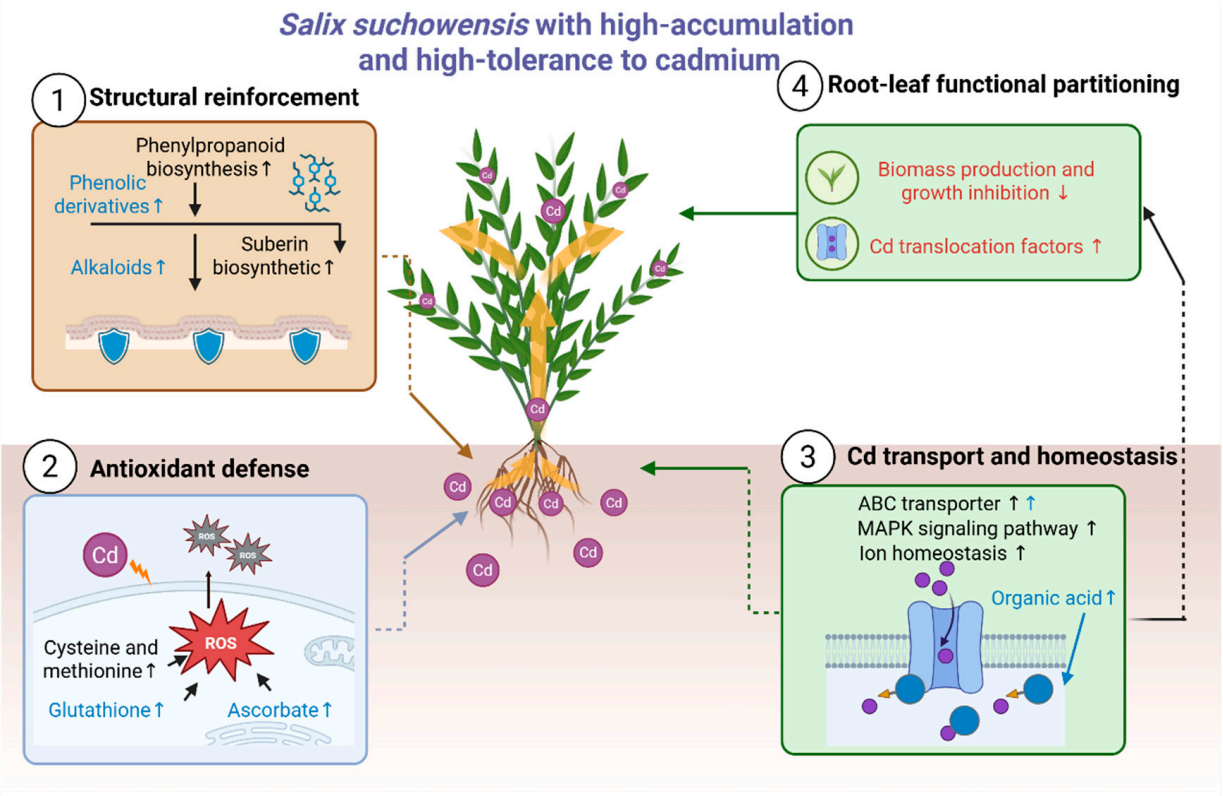

Figure 5. Integrated model illustrating the coordinated mechanisms underlying cadmium tolerance and accumulation in *Salix*. The schematic summarizes transcriptomic and metabolomic evidence from the Cd-tolerant *Salix* genotype P294. Roots serve as the primary detoxification and regulatory hub, integrating multiple defense layers: (1) Phenylpropanoid and suberin/wax biosynthesis strengthen structural barriers in response to Cd stress (black solid arrows indicate the direction of metabolite biosynthesis). (2) Enhanced cysteine methionine metabolism, glutathione and ascorbate enhance antioxidant defense induced by Cd stress. (3) Enhanced ABC transporters, MAPK signaling, and ion homeostasis mediate Cd efflux and vacuolar sequestration. (4) Cd-tolerant *Salix* exhibits integrated root–leaf functional partitioning, where roots mediate Cd uptake and translocation, while leaves contribute to Cd stabilization and detoxification, ensuring efficient whole-plant tolerance. Purple circles represent Cd; black text indicates transcriptionally upregulated pathways; blue text indicates metabolically enriched pathways; yellow arrows show Cd transport directions.

4. Discussion

Cd tolerance and accumulation are two key traits determining the phytoremediation potential of woody plants [17]. While most genotypes exhibit either tolerance or accumulation, the coexistence of both traits is rare and highly desirable for effective phytoremediation [5,43]. In this study, we demonstrated that the *Salix* genotype P294 represented a unique "high-accumulation and high-tolerance" phenotype, maintaining superior root growth and biomass under Cd stress while translocating substantial amounts of Cd to aboveground tissues (Figure 1). Such strategies have been reported in other *Salix* clones, where high-Cd accumulators display greater translocation factors and maintain productivity under stress [32]. Correspondingly, we found both from the transcriptomic and metabolomic data that roots of the tolerant genotype P294 exhibited a much stronger and broader response to Cd stress than leaves. This pattern was consistent with observations in other phytoremediation species such as *Apocynum venetum* [44] and *Arundo donax* [45], where roots acted as the frontline defense in Cd detoxification and changed multiple functions in response to Cd stress. In the tolerant genotype P294, the root response appeared to integrate multiple defense layers, including antioxidant activation, transporter-mediated

Cd efflux, and structural barrier enhancement. Such coordinated regulation allowed roots not only to detoxify Cd locally but also to maintain ion homeostasis and facilitate Cd redistribution to stems, thereby preventing overaccumulation in sensitive root tissues [15,46]. Meanwhile, the leaves of the tolerant genotype also showed transcriptional activation of flavonoid and phenolic metabolism, suggesting that aboveground tissues cooperatively mitigate Cd-induced oxidative pressure once translocated metals reach aerial organs [47]. From a horticultural perspective, the identification of Cd-tolerant and high-accumulating *Salix* genotypes provides useful insights for selecting woody plants suitable for landscaping and green infrastructure in contaminated environments [48]. Such traits are particularly relevant for sustainable horticultural practices in urban and peri-urban systems.

Integrated transcriptomic and metabolomic analyses revealed several connected pathways consistently activated in the Cd-tolerant *Salix* roots, highlighting their central roles in forming Cd tolerance and accumulation. For example, cysteine and methionine metabolism, involved in sulfur assimilation [49,50], was enriched transcriptionally in tolerant roots (Figure 2), aligning with elevated metabolite levels of amino acids and organic acids (Figure 4). These results suggested the Cd-tolerant genotype enhanced their redox buffering [51,52] and metal chelation [53,54] in roots. Similar stress adaptation strategies have also been reported in other resilient plant genotypes under abiotic stress conditions, including enhanced antioxidant enzyme activity and the accumulation of osmolytes and stress-related metabolites, which contribute to maintaining cellular homeostasis during early stress exposure [55]. Concurrently, phenylpropanoid biosynthesis and suberin/wax/cutin synthesis were upregulated, and secondary metabolites such as phenolic acids, flavonoids, and alkaloids accumulated; these together suggest that *Salix* P294 roots employ both chemical defenses (chelation, antioxidants) [56] and physical barriers (structural reinforcements) [57,58] to defend Cd stress (Figure 4). Similar dual strategies have been reported in *Populus* × *canescens*, where exogenous glutathione boosted both Cd uptake and antioxidant responses alongside transporter gene expression [59]. Also, in *Sedum alfredii*, where hyperaccumulating genotype localized Cd in stem parenchyma and associated it with malate and other organic acid ligands, coupled with strong phenylpropanoid metabolism and structural sequestration in vacuoles [60]. These evidences emphasized that these associated metabolic and structural pathways were not incidental but essential supporting modules to sustain tolerant performance under Cd stress.

ABC transporters stand out in our study as the core KEGG pathway commonly enriched in both transcriptome and metabolome data (Figures 2 and 4), highlighting its importance in Cd tolerance and accumulation. In tolerant roots, upregulated ABC transporter genes, alongside enhanced levels of glutathione-related and organic acid metabolites, imply active efflux [61] or vacuolar sequestration of Cd-ligand complexes [62]. The observed dominance of ion transport and glutathione-related detoxification pathways aligns with the general mechanisms reported in a wide range of Cd-tolerant plants, indicating a degree of evolutionary conservation. For instance, in *Populus tomentosa*, PtoABCG36 functions as a plasma membrane Cd extrusion pump and confers increased Cd tolerance; overexpression reduces root Cd accumulation and improves shoot growth under Cd stress [63]. Also, in *Populus* × *canescens*, external glutathione application enhances expression of ABC transporters and increases Cd accumulation in aerial parts while reducing oxidative damage in roots [59]. These conserved pathways across genotypes highlights that Cd tolerance is built upon a shared molecular framework, within which genotype-specific enhancements confer differential resilience and accumulation capacities. Beyond these conserved responses, several tolerance-specific pathways were identified that distinguished P294 from the susceptible genotype. Notably, MAPK signaling, ether lipid metabolism, and flavonoid biosynthesis were markedly upregulated in tolerant roots and leaves but absent or weakly

expressed in the susceptible line (Figure 4). MAPK signaling cascades are known to mediate stress perception and transcriptional reprogramming under Cd stress [64], suggesting that enhanced signaling sensitivity may enable faster and more coordinated Cd responses in P294. Ether lipid metabolism, which contributes to membrane stabilization [65], has rarely been discussed in woody Cd-tolerant genotypes but could play an important role in maintaining membrane integrity under oxidative stress. These tolerance-specific pathways therefore represent distinct regulatory modules that enhance both Cd resistance and translocation efficiency in *Salix*, expanding the current understanding of woody plant adaptation to metal stress.

Our study provides a controlled framework for investigating Cd responses in *Salix*, though several aspects could be further expanded in future work. First, although high and consistent mapping rates were obtained across samples, potential biases caused by sequence variation between genotypes and the reference genome cannot be completely excluded. Future studies could incorporate SNP-aware alignment strategies or pan-transcriptome references to further minimize such biases and improve quantification accuracy. Second, this study focused on a single Cd concentration and exposure duration, representing a biologically relevant and well-defined stress condition [28]. It may not fully capture the dynamic and dose-dependent nature of Cd responses in *Salix*. Future studies incorporating multiple Cd levels and time-course analyses would provide a more comprehensive understanding of the regulatory networks underlying Cd tolerance and accumulation. Third, this study was conducted under controlled hydroponic conditions, which provide a simplified and reproducible system for mechanistic investigation. Although this design facilitates controlled comparisons and mechanistic insights, they do not fully reflect the complexity of soil environments. Future studies incorporating field trials, phenological observations, and long-term performance evaluation will be necessary to further validate the horticultural applicability of these findings. Finally, the primary objective of this study was to establish robust gene expression–metabolite–phenotype associations through multi-omics integration to generate prioritized candidates for subsequent functional characterization. Ongoing and future work will focus on functional validation using approaches such as gene overexpression, RNA interference, and genome editing (e.g., CRISPR/Cas systems) to elucidate the specific roles of these genes in Cd uptake, transport, and detoxification.

5. Conclusions

Our findings provide insights into transcriptional and metabolic responses associated with Cd tolerance in *Salix*. The tolerant genotype P294 exhibited a coordinated response patterns that integrated redox buffering, structural reinforcement, and transporter-mediated detoxification at the root level, while maintaining active allocation and antioxidative protection in leaves. The convergence of transcriptomic and metabolomic evidence underscored that Cd tolerance was not governed by a single pathway but arose from a multi-layered regulatory network, balancing detoxification, transport, and metabolic homeostasis. This integrated strategy allowed *Salix* to simultaneously tolerate and accumulate Cd, representing an adaptive advantage for phytoremediation. The identification of both conserved and *Salix* specific pathways, particularly those involving MAPK signaling and ether lipid metabolism, extended current models of Cd stress adaptation in woody plants and may provide potential molecular targets for improving phytoremediation efficiency through genetic or microbial interventions.

Supplementary Materials: The following supporting information can be downloaded at: https://www.mdpi.com/article/10.3390/horticulturae12040473/s1. Figure S1: Comparison of Cd translocation factors from root to stem and to leaf between two *Salix* genotypes; Figure S2: The expression patterns of differentially expressed genes (DEGs) identified by RNA-Seq using RT-qPCR; Table S1: Primers used for RT-qPCR analysis; Table S2: Identified differential expressed genes in response to cadmium stress for the tolerant and susceptible genotypes in roots and leaves; Table S3: Identified differential expressed metabolites in response to cadmium stress for the tolerant and susceptible genotypes in roots and leaves.

Author Contributions: Conceptualization, N.G. and J.T.; methodology, X.S. and N.W.; software, X.S. and N.W.; validation, Y.Z. and X.H.; formal analysis, X.S., N.W. and Y.Z.; resources, X.H.; writing—original draft preparation, X.S. and N.W.; writing—review and editing, N.G. and J.T.; visualization, X.S. and N.W.; supervision, N.G. and J.T.; project administration, J.T.; funding acquisition, N.G. and J.T. All authors have read and agreed to the published version of the manuscript.

Funding: This research was funded by the Independent Research Project of Jiangsu Academy of Forestry, grant number ZZKY202101, and Jiangsu Province Innovation and Extension Project of Forestry Science and Technology of China, grant number LYKJ[2023]16).

Data Availability Statement: The original data presented in the study are openly available in NCBI SRA database at https://www.ncbi.nlm.nih.gov/ (accessed on 26 March 2026) or Bio Project ID: PRJNA1437169.

Conflicts of Interest: The authors declare no conflicts of interest.

References

1. Rahman, Z.; Singh, V.P. The relative impact of toxic heavy metals (THMs) (arsenic (As), cadmium (Cd), chromium (Cr)(VI), mercury (Hg), and lead (Pb)) on the total environment: An overview. *Environ. Monit. Assess.* **2019**, *191*, 419. [CrossRef]
2. Satarug, S.; Baker, J.R.; Urbenjapol, S.; Haswell-Elkins, M.; Reilly, P.E.B.; Williams, D.J.; Moore, M.R. A global perspective on cadmium pollution and toxicity in non-occupationally exposed population. *Toxicol. Lett.* **2003**, *137*, 65–83. [CrossRef] [PubMed]
3. Aslam, M.M.; Okal, E.J.; Waseem, M. Cadmium toxicity impacts plant growth and plant remediation strategies. *Plant Growth Regul.* **2023**, *99*, 397–412. [CrossRef]
4. Liu, L.W.; Li, W.; Song, W.P.; Guo, M.X. Remediation techniques for heavy metal-contaminated soils: Principles and applicability. *Sci. Total Environ.* **2018**, *633*, 206–219. [CrossRef] [PubMed]
5. Sarwar, N.; Imran, M.; Shaheen, M.R.; Ishaque, W.; Kamran, M.A.; Matloob, A.; Rehim, A.; Hussain, S. Phytoremediation strategies for soils contaminated with heavy metals: Modifications and future perspectives. *Chemosphere* **2017**, *171*, 710–721. [CrossRef]
6. Vandecasteele, B.; Meers, E.; Vervaeke, P.; Vos, B.D.; Quataert, P.; Tack, F.M.G. Growth and trace metal accumulation of two *Salix* clones on sediment-derived soils with increasing contamination levels. *Chemosphere* **2005**, *58*, 995–1002. [CrossRef]
7. Zacchini, M.; Pietrini, F.; Scarascia Mugnozza, G.; Iori, V.; Pietrosanti, L.; Massacci, A. Metal tolerance, accumulation and translocation in poplar and willow clones treated with cadmium in hydroponics. *Water Air Soil Pollut.* **2009**, *197*, 23–34. [CrossRef]
8. Cao, Y.; Tan, Q.; Zhang, F.; Ma, C.; Xiao, J.; Chen, G. Phytoremediation potential evaluation of multiple *Salix* clones for heavy metals (Cd, Zn and Pb) in flooded soils. *Sci. Total Environ.* **2022**, *813*, 152482. [CrossRef]
9. Karp, A.; Hanley, S.J.; Trybush, S.O.; Macalpine, W.; Pei, M.; Shield, I. Genetic improvement of willow for bioenergy and biofuels. *J. Integr. Plant Biol.* **2011**, *53*, 151–165. [CrossRef]
10. Kuzovkina, Y.A.; Quigley, M.F. Ornamental Willows (*Salix* spp.) For alpine and small urban gardens. *Arboric. Urban For.* **2004**, *30*, 127–132. [CrossRef]
11. Roviello, G.N. The multifunctional role of *Salix* spp.: Linking phytoremediation, forest therapy, and phytomedicine for environmental and human benefits. *Forests* **2025**, *16*, 1808. [CrossRef]
12. Tőzsér, D.; Magura, T.; Simon, E. Heavy metal uptake by plant parts of willow species: A meta-analysis. *J. Hazard. Mater.* **2017**, *336*, 101–109. [CrossRef]
13. Mleczek, M.; Rutkowski, P.; Rissmann, I.; Kaczmarek, Z.; Golinski, P.; Szentner, K.; Strażyńska, K.; Stachowiak, A. Biomass productivity and phytoremediation potential of *Salix alba* and *Salix viminalis*. *Biomass Bioenergy* **2010**, *34*, 1410–1418. [CrossRef]
14. Dos Santos Utmazian, M.N.; Wenzel, W.W. Cadmium and zinc accumulation in willow and poplar species grown on polluted soils. *J. Plant Nutr. Soil. Sci.* **2007**, *170*, 265–272. [CrossRef]

15. Haider, F.U.; Liqun, C.; Coulter, J.A.; Cheema, S.A.; Wu, J.; Zhang, R.; Wenjun, M.; Farooq, M. Cadmium toxicity in plants: Impacts and remediation strategies. *Ecotoxicol. Environ. Saf.* **2021**, *211*, 111887. [CrossRef]
16. Niu, L.; Li, C.; Wang, W.; Zhang, J.; Scali, M.; Li, W.; Liu, H.; Tai, F.; Hu, X.; Wu, X. Cadmium tolerance and hyperaccumulation in plants—A proteomic perspective of phytoremediation. *Ecotoxicol. Environ. Saf.* **2023**, *256*, 114882. [CrossRef]
17. Luo, Z.-B.; He, J.; Polle, A.; Rennenberg, H. Heavy metal accumulation and signal transduction in herbaceous and woody plants: Paving the way for enhancing phytoremediation efficiency. *Biotechnol. Adv.* **2016**, *34*, 1131–1148. [CrossRef]
18. Yang, W.D.; Zhao, F.L.; Zhang, X.C.; Ding, Z.L.; Wang, Y.Y.; Zhu, Z.Q.; Yang, X.E. Variations of cadmium tolerance and accumulation among 39 *Salix* clones: Implications for phytoextraction. *Environ. Earth Sci.* **2015**, *73*, 3263–3274. [CrossRef]
19. Küpper, H.; Lombi, E.; Zhao, F.-J.; McGrath, S.P. Cellular compartmentation of cadmium and zinc in relation to other elements in the hyperaccumulator *Arabidopsis halleri*. *Planta* **2000**, *212*, 75–84. [CrossRef] [PubMed]
20. Cobbett, C.; Goldsbrough, P. Phytochelatins and metallothioneins: Roles in heavy metal detoxification and homeostasis. *Annu. Rev. Plant Biol.* **2002**, *53*, 159–182. [CrossRef]
21. Kim, D.-Y.; Bovet, L.; Maeshima, M.; Martinoia, E.; Lee, Y. The ABC transporter AtPDR8 is a cadmium extrusion pump conferring heavy metal resistance. *Plant J.* **2007**, *50*, 207–218. [CrossRef] [PubMed]
22. Park, W.; Ahn, S.-J. HMA3 is a key factor for differences in Cd- and Zn-related phenotype between Arabidopsis Ws and Col-0 ecotypes. *Plant Biotechnol. Rep.* **2017**, *11*, 209–218. [CrossRef]
23. Cornu, J.Y.; Deinlein, U.; Höreth, S.; Braun, M.; Schmidt, H.; Weber, M.; Persson, D.P.; Husted, S.; Schjoerring, J.K.; Clemens, S. Contrasting effects of nicotianamine synthase knockdown on zinc and nickel tolerance and accumulation in the zinc/cadmium hyperaccumulator *Arabidopsis halleri*. *New. Phytol.* **2015**, *206*, 738–750. [CrossRef]
24. Rizwan, M.; Ali, S.; Adrees, M.; Ibrahim, M.; Tsang, D.C.W.; Zia-ur-Rehman, M.; Zahir, Z.A.; Rinklebe, J.; Tack, F.M.G.; Ok, Y.S. A critical review on effects, tolerance mechanisms and management of cadmium in vegetables. *Chemosphere* **2017**, *182*, 90–105. [CrossRef]
25. Zhao, F.-J.; Tang, Z.; Song, J.-J.; Huang, X.-Y.; Wang, P. Toxic metals and metalloids: Uptake, transport, detoxification, phytoremediation, and crop improvement for safer food. *Mol. Plant* **2022**, *15*, 27–44. [CrossRef]
26. Clemens, S.; Ma, J.F. Toxic heavy metal and metalloid accumulation in crop plants and foods. *Annu. Rev. Plant Biol.* **2016**, *67*, 489–512. [CrossRef]
27. Han, X.; Zhang, Y.; Yu, M.; Zhang, J.; Xu, D.; Lu, Z.; Qiao, G.; Qiu, W.; Zhuo, R. Transporters and ascorbate–glutathione metabolism for differential cadmium accumulation and tolerance in two contrasting willow genotypes. *Tree Physiol.* **2020**, *40*, 1126–1142. [CrossRef]
28. Guo, N.; Fan, L.; Cao, Y.; Ling, H.; Xu, G.; Zhou, J.; Chen, Q.; Tao, J. Comparison of two willow genotypes reveals potential roles of *iron-regulated transporter 9* and *heavy-metal ATPase 1* in cadmium accumulation and resistance in *Salix suchowensis*. *Ecotoxicol. Environ. Saf.* **2022**, *244*, 114065. [CrossRef]
29. Jiang, Y.; Han, J.; Xue, W.; Wang, J.; Wang, B.; Liu, L.; Zou, J. Overexpression of SmZIP plays important roles in Cd accumulation and translocation, subcellular distribution, and chemical forms in transgenic tobacco under Cd stress. *Ecotoxicol. Environ. Saf.* **2021**, *214*, 112097. [CrossRef]
30. Guo, N.; Ling, H.; Yu, R.; Gao, F.; Cao, Y.; Tao, J. Expression of *Sailx suchowensis* SsIRT9 enhances cadmium accumulation and alters metal homeostasis in tobacco. *J. Hazard. Mater.* **2024**, *463*, 132958. [CrossRef] [PubMed]
31. Yang, J.; Li, K.; Zheng, W.; Zhang, H.; Cao, X.; Lan, Y.; Yang, C.; Li, C. Characterization of early transcriptional responses to cadmium in the root and leaf of Cd-resistant *Salix matsudana* Koidz. *BMC Genom.* **2015**, *16*, 705. [CrossRef]
32. Song, X.; Wang, N.; Zhou, J.; Tao, J.; He, X.; Guo, N. High cadmium-accumulating *Salix* ecotype shapes rhizosphere microbiome to facilitate cadmium extraction. *Environ. Int.* **2024**, *190*, 108904. [CrossRef]
33. Song, X.; Guo, N.; Yu, R.; Huang, R.; Zhang, K.; Chen, Q.; Tao, J. Assessment of the capability of cadmium accumulation and translocation among 31 willows: Four patterns of willow biomass variation response to cadmium. *Environ. Sci. Pollut. Res.* **2023**, *30*, 76735–76745. [CrossRef] [PubMed]
34. Chen, S.; Zhou, Y.; Chen, Y.; Gu, J. Fastp: An ultra-fast all-in-one FASTQ preprocessor. *Bioinformatics* **2018**, *34*, i884–i890. [CrossRef]
35. Kim, D.; Langmead, B.; Salzberg, S.L. HISAT: A fast spliced aligner with low memory requirements. *Nat. Methods* **2015**, *12*, 357–360. [CrossRef] [PubMed]
36. Pertea, M.; Pertea, G.M.; Antonescu, C.M.; Chang, T.-C.; Mendell, J.T.; Salzberg, S.L. StringTie enables improved reconstruction of a transcriptome from RNA-seq reads. *Nat. Biotechnol.* **2015**, *33*, 290–295. [CrossRef]
37. Wang, N.; Li, Y.; Han, S.; Zhang, Y.; Yang, J.; Yin, Z.; Deng, C.; Liu, Z.; Wu, Y.; Wu, W.; et al. CFViSA: A comprehensive and free platform for visualization and statistics in omics-data. *Comput. Biol. Med.* **2024**, *171*, 108206. [CrossRef]

38. Huang, L.; Zhang, Y.; Gao, F.; Fu, Y.; Sun, J.; Zhou, J.; Tao, J.; He, X.; Guo, N. *EF1α* and *αTUB* are stable reference gene pairs for RT-qPCR-based gene expression studies in *Salix suchowensis* under nitrogen treatment conditions. *Plants* **2025**, *14*, 19. [CrossRef] [PubMed]
39. Chen, W.; Gong, L.; Guo, Z.; Wang, W.; Zhang, H.; Liu, X.; Yu, S.; Xiong, L.; Luo, J. A novel integrated method for large-scale detection, identification, and quantification of widely targeted metabolites: Application in the study of rice metabolomics. *Mol. Plant* **2013**, *6*, 1769–1780. [CrossRef]
40. Pang, Z.; Xu, L.; Viau, C.; Lu, Y.; Salavati, R.; Basu, N.; Xia, J. MetaboAnalystR 4.0: A unified LC-MS workflow for global metabolomics. *Nat. Commun.* **2024**, *15*, 3675. [CrossRef]
41. Dixon, P. VEGAN, a package of R functions for community ecology. *J. Veg. Sci.* **2003**, *14*, 927–930. [CrossRef]
42. Love, M.I.; Huber, W.; Anders, S. Moderated estimation of fold change and dispersion for RNA-seq data with DESeq2. *Genome Biol.* **2014**, *15*, 550. [CrossRef]
43. Ali, H.; Khan, E.; Sajad, M.A. Phytoremediation of heavy metals—Concepts and applications. *Chemosphere* **2013**, *91*, 869–881. [CrossRef]
44. Jing, C.; Wang, M.; Lu, X.; Prince, M.; Zhang, M.; Li, Y.; Zhang, C.; Meng, C.; Zhang, L.; Zheng, Y.; et al. Transcriptome analysis reveals how cadmium promotes root development and accumulates in *Apocynum venetum*, a promising plant for greening cadmium-contaminated soil. *Ecotoxicol. Environ. Saf.* **2024**, *270*, 115872. [CrossRef]
45. Santoro, D.F.; Sicilia, A.; Testa, G.; Cosentino, S.L.; Lo Piero, A.R. Global leaf and root transcriptome in response to cadmium reveals tolerance mechanisms in *Arundo donax* L. *BMC Genom.* **2022**, *23*, 427. [CrossRef]
46. Podar, D.; Maathuis, F.J.M. The role of roots and rhizosphere in providing tolerance to toxic metals and metalloids. *Plant Cell. Environ.* **2022**, *45*, 719–736. [CrossRef]
47. Karabourniotis, G.; Liakopoulos, G.; Nikolopoulos, D.; Bresta, P. Protective and defensive roles of non-glandular trichomes against multiple stresses: Structure–function coordination. *J. For. Res.* **2020**, *31*, 1–12. [CrossRef]
48. Kuzovkina, Y.A.; Volk, T.A. The characterization of willow (*Salix* L.) varieties for use in ecological engineering applications: Co-ordination of structure, function and autecology. *Ecol. Eng.* **2009**, *35*, 1178–1189. [CrossRef]
49. Leustek, T.; Martin, M.N.; Bick, J.-A.; Davies, J.P. Pathways and regulation of sulfur metabolism revealed through molecular and genetic studies. *Annu. Rev. Plant Biol.* **2000**, *51*, 141–165. [CrossRef] [PubMed]
50. Liang, J.; Shohag, M.J.I.; Yang, X.; Tian, S.; Zhang, Y.; Feng, Y.; He, Z. Role of sulfur assimilation pathway in cadmium hyperaccumulation by Sedum alfredii Hance. *Ecotoxicol. Environ. Saf.* **2014**, *100*, 159–165. [CrossRef] [PubMed]
51. Collado-Arenal, A.M.; Exposito-Rodriguez, M.; Mullineaux, P.M.; Olmedilla, A.; Romero-Puertas, M.C.; Sandalio, L.M. Cadmium exposure induced light/dark- and time-dependent redox changes at subcellular level in Arabidopsis plants. *J. Hazard. Mater.* **2024**, *477*, 135164. [CrossRef] [PubMed]
52. Gruhlke, M.C.H.; Slusarenko, A.J. The biology of reactive sulfur species (RSS). *Plant Physiol. Biochem.* **2012**, *59*, 98–107. [CrossRef] [PubMed]
53. Wang, L.; Li, R.; Yan, X.; Liang, X.; Sun, Y.; Xu, Y. Pivotal role for root cell wall polysaccharides in cultivar-dependent cadmium accumulation in *Brassica chinensis* L. *Ecotoxicol. Environ. Saf.* **2020**, *194*, 110369. [CrossRef]
54. Liao, Q.; Xiao, H.; Chen, L.; Shen, C.; Wang, B.; Zhou, W.; Fu, H.; Zheng, Z.; Huang, B.; Xin, J.; et al. Potassium alters cadmium accumulation and translocation by regulating root cell wall biosynthesis in Brassica napus. *Sci. Hortic.* **2025**, *339*, 113833. [CrossRef]
55. Ait Hammou, R.; Ben El Caid, M.; Harrouni, C.; Daoud, S. Germination enhancement, antioxidant enzyme activity, and metabolite changes in late Argania spinosa kernels under salinity. *J. Arid. Environ.* **2023**, *219*, 105095. [CrossRef]
56. Arnao, M.B.; Cano, A.; Acosta, M. The hydrophilic and lipophilic contribution to total antioxidant activity. *Food Chem.* **2001**, *73*, 239–244. [CrossRef]
57. Mahmood, S.; Wahid, A.; Azeem, M.; Zafar, S.; Bashir, R.; Bajwa, M.O.S.; Ali, S. Tyrosine or lysine priming modulated phenolic metabolism and improved cadmium stress tolerance in mung bean (*Vigna radiata* L.). *S. Afr. J. Bot.* **2022**, *149*, 397–406. [CrossRef]
58. Vogt, T. Phenylpropanoid biosynthesis. *Mol. Plant* **2010**, *3*, 2–20. [CrossRef]
59. Ding, S.; Ma, C.; Shi, W.; Liu, W.; Lu, Y.; Liu, Q.; Luo, Z.-B. Exogenous glutathione enhances cadmium accumulation and alleviates its toxicity in Populus × canescens. *Tree Physiol.* **2017**, *37*, 1697–1712. [CrossRef] [PubMed]
60. Tian, S.; Lu, L.; Labavitch, J.; Yang, X.; He, Z.; Hu, H.; Sarangi, R.; Newville, M.; Commisso, J.; Brown, P. Cellular sequestration of cadmium in the hyperaccumulator plant species *Sedum alfredii*. *Plant Physiol.* **2011**, *157*, 1914–1925. [CrossRef]
61. Fu, S.; Lu, Y.; Zhang, X.; Yang, G.; Chao, D.; Wang, Z.; Shi, M.; Chen, J.; Chao, D.-Y.; Li, R.; et al. The ABC transporter ABCG36 is required for cadmium tolerance in rice. *J. Exp. Bot.* **2019**, *70*, 5909–5918. [CrossRef] [PubMed]
62. Park, J.; Song, W.-Y.; Ko, D.; Eom, Y.; Hansen, T.H.; Schiller, M.; Lee, T.G.; Martinoia, E.; Lee, Y. The phytochelatin transporters AtABCC1 and AtABCC2 mediate tolerance to cadmium and mercury. *Plant J.* **2012**, *69*, 278–288. [CrossRef]
63. Wang, H.; Liu, Y.; Peng, Z.; Li, J.; Huang, W.; Liu, Y.; Wang, X.; Xie, S.; Sun, L.; Han, E.; et al. Ectopic Expression of poplar ABC transporter PtoABCG36 confers Cd tolerance in *Arabidopsis thaliana*. *Int. J. Mol. Sci.* **2019**, *20*, 3293. [CrossRef]

64. Jalmi, S.K.; Bhagat, P.K.; Verma, D.; Noryang, S.; Tayyeba, S.; Singh, K.; Sharma, D.; Sinha, A.K. Traversing the links between heavy metal stress and plant signaling. *Front. Plant Sci.* **2018**, *9*, 12. [CrossRef] [PubMed]
65. Dean, J.M.; Lodhi, I.J. Structural and functional roles of ether lipids. *Protein Cell* **2018**, *9*, 196–206. [CrossRef] [PubMed]

Disclaimer/Publisher's Note: The statements, opinions and data contained in all publications are solely those of the individual author(s) and contributor(s) and not of MDPI and/or the editor(s). MDPI and/or the editor(s) disclaim responsibility for any injury to people or property resulting from any ideas, methods, instructions or products referred to in the content.